

RESEARCH

Open Access



# Design and validation of an alignment free adaptive joint torque measurement system

Lei Li<sup>1,2</sup>, Jingcheng Chen<sup>3</sup>, Shaoming Sun<sup>1,3\*</sup> and Wei Peng<sup>1,3\*</sup>

\*Correspondence:  
ssmjkcjzll@outlook.com;  
wpeng@iim.ac.cn

<sup>1</sup> Hefei Institutes of Physical Science, Chinese Academy of Sciences, 350 Shushan Lake Road, Hefei 230031, China

<sup>2</sup> University of Science and Technology of China, Hefei 230026, China

<sup>3</sup> CAS Hefei Institute of Technology Innovation, Hefei 230088, China

## Abstract

**Purpose:** This study introduces a transferable alignment-free adaptive joint torque measurement (AFAJTM) system designed to resolve inconsistencies in torque measurements caused by misalignment between dynamometer and joint rotational axes, improving accuracy and reliability in joint torque assessment.

**Method:** This study presents the design and control methodology of an alignment free adaptive joint torque measurement system. An elbow joint torque measurement device (EJTMD) was developed, and its torque consistency and repeatability were evaluated at various misalignment positions using a joint simulation model. Clinical experiments compared torque measurements between the EJTMD and a traditional standard dynamometer during maximum voluntary contraction (MVC) tests at different misalignment positions.

**Result:** The simulation test results demonstrate that the AFAJTM system can achieve high-precision torque measurements, with measurement errors controlled within  $\pm 0.5$  Nm at various misalignment positions. Clinical experiment data show that the EJTMD exhibits high consistency in torque measurements compared to the traditional standard dynamometer across five different misalignment positions, with strong repeatability and reliability.

**Conclusion:** The AFAJTM system provides a novel solution for joint torque measurement under human-machine axis misalignment conditions, a solution that eliminates the need for axis alignment, effectively overcoming the limitations of traditional measurement devices. This system can be widely applied in various devices that require joint torque measurement, demonstrating excellent adaptability and high-precision measurement capabilities.

**Keywords:** Human-machine, Misalignment, Alignment-free, Adaptability, Joint torque, Measurement, Automatically, MVC test, Dynamometer, Rehabilitation

## Introduction

Accurate assessment of the human musculoskeletal system performance has long been a key goal for scientists and practitioners in the fields of physical medicine and rehabilitation. In the field of rehabilitation, muscle strength measurement can quantify the extent of injury [1, 2] and monitor patients' recovery during the rehabilitation process [3–5]. In



sports medicine, joint torque assessment provides a scientific basis for optimizing athletic performance [6–8].

Joint torque measurement methods are typically classified into manual and automated device-based techniques. Manual methods typically use handheld force measurement devices with torque sensors to assess passive joint resistance during isometric movements of the limbs [9, 10]. This method relies on the examiner's experience and lacks standardized procedures, making it difficult to cover a wide range of activities or high-speed movements [11], and it is unreliable for measuring end range of motion and peak torque angles [12], with measurement errors insufficient for individual-level assessments [13]. In contrast, automated measurements collect joint forces and kinematic data, providing more objective and precise results [11, 14, 15]. Furthermore, automated systems support various measurement modes (such as isometric, isotonic, isokinetic, active and passive mode), which significantly address the limitations of manual measurements [16–18].

The Cybex Norm (Cybex, Ronkonkoma, New York), Biodex System (Biodex, Shirley, New York) and IsoMed (D&R Ferstl GmbH, Hemau, Germany) dynamometer is a commercially available standard device widely used in rehabilitation and sports science for assessing joint torque and muscle strength [19, 20]. Current automated measurement devices typically require the rotational axis of the joint under test to be strictly aligned with the drive axis of the equipment [11]. As a result, before each test, the tester must carefully adjust the position of the participant relative to the dynamometer [8]. However, due to the flexibility of the dynamometer components (such as the seat and connection pads) and the deformation of human soft tissues, perfect alignment between the two axes is impossible. Therefore, some measurement errors in joint torque are unavoidable [8, 21]. Existing manual alignment methods not only increase preparation time but are also prone to subjective influence, leading to inevitable alignment errors [11]. Any misalignment between joint axis and the dynamometer axis can not only cause discomfort but also result in damage to the joint or skin, and lead to biased torque measurements. MajidiRad A H [21] found that the misalignment between the exoskeleton and the knee joint leads to significant changes in muscle stress, which refers to variations in muscle force caused by joint misalignment. For example, a 5 mm lateral offset from an anatomically healthy knee joint location resulted in a 4.3% increase in the force generated by the Vastus lateralis muscle. Additionally, during circular shank trajectories supported by the exoskeleton, muscle strain variations were observed in the Rectus femoris (44%), Biceps femoris long head (32%), and Gastrocnemius muscles (31–33%). These alterations may adversely affect user safety and rehabilitation outcomes. Houweling T A W [22] demonstrated that misalignment of the knee joint relative to the Cybex Norm dynamometer significantly affected the peak knee flexion torque, with errors ranging from 21 to 29%. Reimann [23] theoretically demonstrated that knee joint axis misalignment with the dynamometer axis causes moment errors proportional to the percentage of displacement, with a 10% axis shift relative to the segment length resulting in approximately a 10% maximum error in the moment. Arampatzis [24] found that the differences between the actual knee joint moment and the moment measured by dynamometry during isometric knee extension ranged from 0.33% to 17%, with an average difference of 7.3%.

Some studies have theoretically explored the impact of the misalignment between the knee joint axis and the dynamometer axis on joint torque measurement [9]. Numerous researchers have proposed various design methods to compensate for joint misalignment. For example, a novel neuro-exoskeleton robot for elbow joint rehabilitation in stroke patients was proposed [25], which addresses the alignment issue by designing a four-degree-of-freedom (DoF) passive mechanism for anatomical axis alignment. Li G [26] introduced a new spatial self-aligning mechanism for knee exoskeletons to assist stroke patients with both active and passive movements, enhancing user comfort during wear. A planar mechanical four-bar linkage mechanism for exoskeleton devices was presented [27], solving the decoupling problem of joint forces and torques in planar exoskeletons, applicable to force enhancement, endurance improvement, or rehabilitation. However, its limitation lies in its inability to measure joint torque. In addition to these methods of designing new structures, MajidiRad A H suggested that using external skin markers combined with simple video or photonic systems to measure axial misalignment could also improve the accuracy of joint torque measurements by correcting the misalignment of the dynamometer axis [21]. But additional expensive equipment was introduced. Although various studies have proposed methods to address misalignment issues, only a limited number have quantitatively evaluated the impact of joint misalignments in the literature.

In this study, we propose an alignment-free adaptive joint torque measurement system (AFAJTM), which serves as a general, adaptable, and transplantable methodology for joint torque measurement. The AFAJTM system incorporates an adjustable linkage that seamlessly integrates with the limb as a unified structure, ensuring perpendicularity to the measured limb and thereby eliminating additional force components caused by alignment discrepancies. This system automatically calculates the joint's axis of rotation based on the geometric and motion constraints defined by the linkage's kinematic relationships, enabling adaptive measurement of joint flexion and extension torques without requiring alignment of the human-machine axes. By fundamentally addressing the human-machine axis misalignment issue in traditional joint torque measurements, AFAJTM offers significant versatility for integration as an independent module into various mechanisms or exoskeleton robots requiring torque measurement. As a demonstration of the AFAJTM system's feasibility, we developed a specific implementation, the Elbow Joint Torque Measurement Device (EJTMD), which utilizes the AFAJTM methodology to achieve accurate joint torque measurement. To validate its performance, we conducted torque measurement consistency verification using a joint simulation model. Additionally, a comparison experiment with the Biodex System in healthy subjects further assessed the accuracy and reliability of the device.

## Results

The Shapiro-Wilk test results indicate that all data follow a normal distribution ( $P > 0.05$ ). The regression model shown in Fig. 1 demonstrates a regression coefficient of 0.99 between the model torque and the EJTMD measured torque, indicating a strong linear relationship ( $P < 0.01$ ) with statistical significance. The coefficient of determination ( $R^2$ ) is 0.993, suggesting a high goodness of fit.

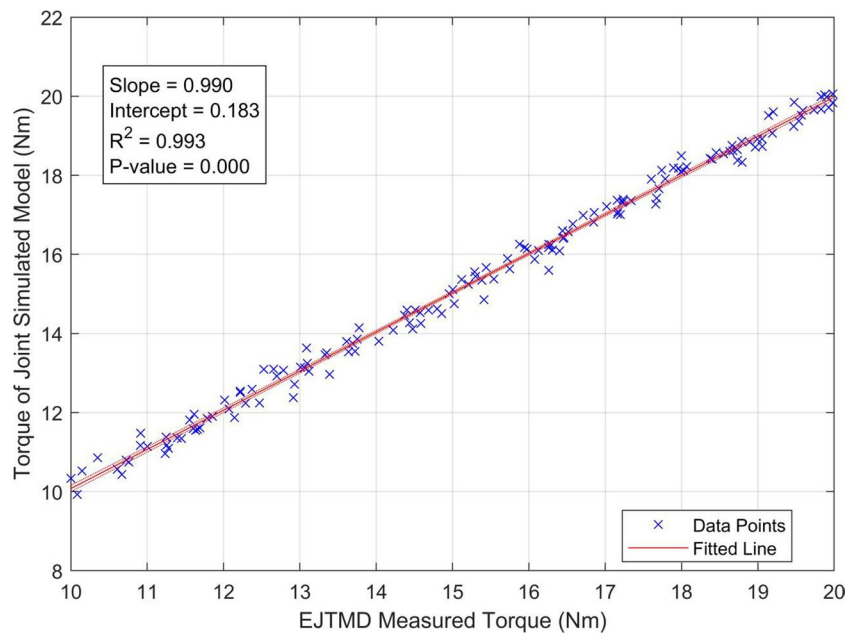


**Fig. 1** Regression analysis of EJTMd torque measurements. Blue "x" marks represent data points, and the red line is the fitted regression line. The slope is 0.990, the intercept is 0.183, the goodness of fit  $R^2$  is 0.993, and the P-value is 0

**Table 1** Torque comparison between EJTMd and simulation model across misalignment positions

Misalignment Position (mm)	EJTMd torque (Mean $\pm$ SD, Nm)	Simulation model (Mean $\pm$ SD, Nm)	R	t-test P-value
- 50,0	14.23 $\pm$ 3.124	14.288 $\pm$ 3.139	0.995	0.510
- 30,0	14.646 $\pm$ 3.086	14.68 $\pm$ 3.085	0.997	0.706
0,0	14.746 $\pm$ 2.904	14.781 $\pm$ 2.908	0.997	0.236
30,0	14.976 $\pm$ 3.106	15.002 $\pm$ 3.03	0.997	0.236
50,0	15.36 $\pm$ 2.507	15.36 $\pm$ 2.496	0.998	0.236

Table 1 presents the measured torque values from the EJTMd at different misalignment positions, the standard torque from the joint simulation model, the Pearson correlation coefficients, and the P-values from the t-tests. The Pearson correlation coefficients between the EJTMd and the simulation model at the five misalignment positions were all greater than 0.99, indicating a very strong linear correlation. However, the t-test p-values for the differences between the measured and simulated torques at each position were all greater than 0.05, suggesting that there are no statistically significant differences between the two sets of values.

Figure 2 illustrates the absolute error distribution between the EJTMd and the Simulation Model. The error distribution is approximately symmetric and centered around zero, indicating that the EJTMd's error is minimal. The red dashed line represents the mean error (- 0.009 Nm), which is close to zero, further confirming the high accuracy of the torque measurements obtained from EJTMd. We also analyzed the impact of force sensor, limb length measurement, and angle measurement errors on the EJTMd torque

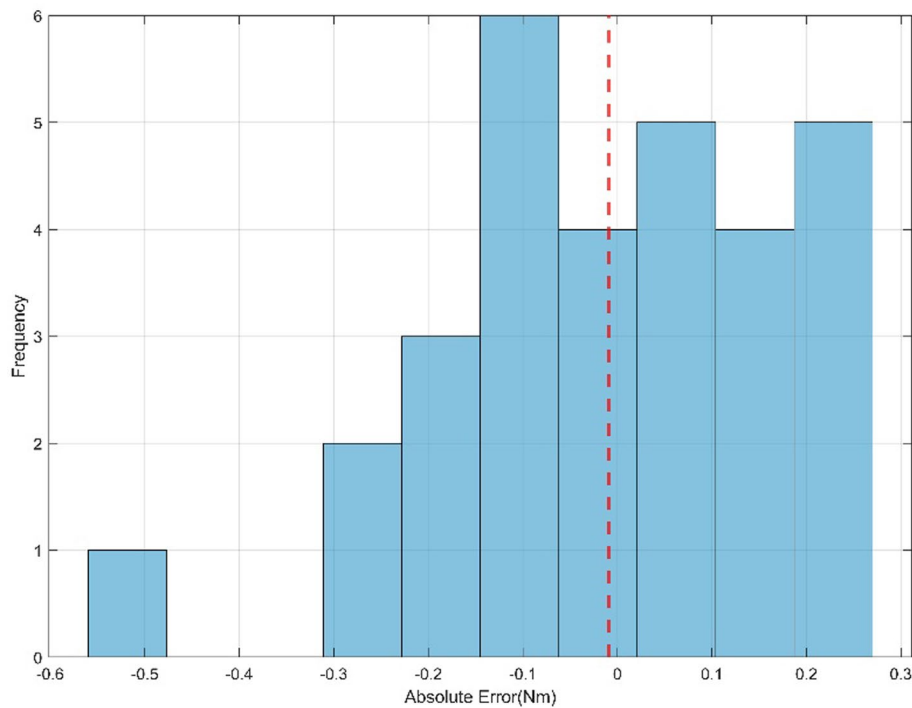


**Fig. 2** Distribution of absolute errors

**Table 2** Clinical comparison of torque measurements from EJTMD and Biodex devices across misalignment positions

Misalignment position (mm)	EJTMD torque (Mean ± SD, Nm)	Biodex torque (Mean ± SD, Nm)
- 50,0	12.373 ± 2.702	14.768 ± 5.140
- 30,0	12.477 ± 2.700	12.832 ± 4.798
0,0	12.289 ± 2.420	10.379 ± 4.631
30,0	12.508 ± 2.695	15.690 ± 5.063
50,0	12.420 ± 2.431	17.343 ± 4.625

measurement. The contribution percentages of each error source are as follows: limb length measurement (93.68%), force sensor (6.32%), and angle measurement (0.0013%).

In the repeated measures ANOVA for the EJTMD torque data, the results show an F-value of 7.564 and a P-value of 0.983, indicating that the difference between positions is not significant. The effect size ( $\eta^2$ ) is 0.033, suggesting that the impact of position differences on the measurement results is minimal. Additionally, the Mauchly’s test for sphericity shows a P-value of 0.973, indicating that the data meets the assumption of sphericity, making the repeated measures ANOVA appropriate for analysis.

Table 2 shows that the mean torque measurements for the EJTMD device ranged from 12.289 to 12.508 Nm across different misalignment positions, with relatively small standard deviations (2.420 to 2.700 Nm), indicating consistent measurements across positions. In contrast, the Biodex system’s torque measurements ranged from 10.379 to 17.343 Nm, with higher standard deviations (4.625 to 5.140 Nm), indicating greater

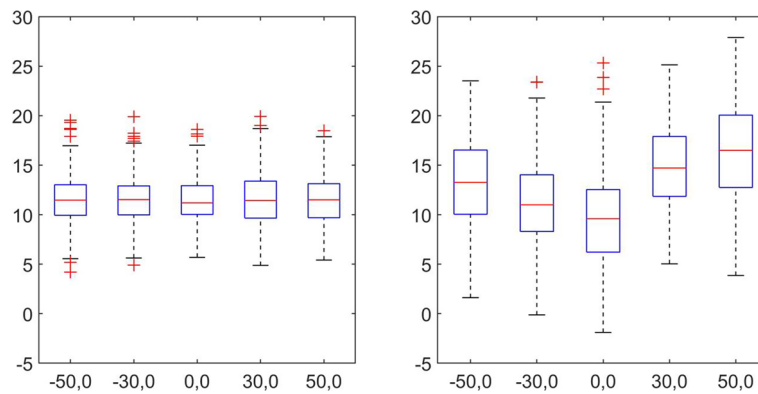


**Fig. 3** Boxplot distribution of torque measurements. **a** EJTMD, **b** Biodex System

**Table 3** Repeated measures ANOVA of the effect of position variations on measurement results by device

Device	F-value	p-value	$\eta^2$	p-value (Mauchly)
EJTMD	0.119	0.979	0.061	0.200
Biodex	46.071	0.001	0.837	0.374

variability in measurements across different misalignment positions. In terms of data dispersion, the coefficient of variation (CV) for the EJTMD ranged from 19.6% to 21.6%, indicating relatively low variability. In contrast, the CV for the Biodex system ranged from 33.4% to 42.4%, showing higher variability and suggesting less consistency in the measurements across the misalignment positions.

Additionally, Fig. 3 visually presents the consistency of the EJTMD and Biodex systems’ measurements at different misalignment positions using box plots.

In this study, three repeated measurements were conducted for the EJTMD at each position, and the intraclass correlation coefficients (ICC) were 0.992, 0.981, 0.973, 0.989, and 0.934, indicating high measurement consistency at all misalignment positions.

As shown in Table 3, the Mauchly’s test results for both devices showed p-values greater than 0.05, indicating no violation of the sphericity assumption, and therefore no correction to the degrees of freedom was required. For the EJTMD, the repeated measures ANOVA showed that position had no significant effect on the measurements ( $F=0.119$ ,  $P=0.979$ ), with a small effect size ( $\eta^2 = 0.061$ ). In contrast, for the Biodex system, the results indicated that position had a significant effect on the measurements ( $F=46.071$ ,  $P<0.001$ ), with a large effect size ( $\eta^2 = 0.837$ ).

Table 4 presents the pairwise comparisons of misalignment position effects on measurement results for the EJTMD and Biodex devices. For the EJTMD device, the P-values for all pairwise comparisons between misalignment positions were greater than 0.99, with the Mean Differences close to zero, indicating no significant differences between the positions. In contrast, for the Biodex device, several pairwise comparisons had p-values significantly lower than 0.05, and the Mean Differences showed large variations, indicating significant differences between the misalignment positions. For example, the comparison between (− 50,0) and (50,0) yielded a p-value of  $<0.001$ , with a Mean

**Table 4** Pairwise comparisons of misalignment position effects on measurement results for EJTMD and bio devices

(I) Position	(J) Position	Mean difference		p-value	
		EJTMD	Biodex	EJTMD	Biodex
- 50,0	- 30,0	- 0.063	2.038	>0.99	0.009
- 50,0	0,0	0.013	3.314	>0.99	0.003
- 50,0	30,0	- 0.004	- 1.435	>0.99	0.151
- 50,0	50,0	- 0.097	- 3.106	>0.99	<0.001
- 30,0	0,0	0.076	1.277	>0.99	0.229
- 30,0	30,0	0.059	- 3.472	>0.99	0.005
- 30,0	50,0	- 0.034	- 5.144	>0.99	<0.001
0,0	30,0	- 0.017	- 4.749	>0.99	<0.001
0,0	50,0	- 0.110	- 6.420	>0.99	<0.001
30,0	50,0	0.093	- 1.672	>0.99	0.015

Difference of 3.106, indicating a significant difference. Overall, the EJTMD showed no significant differences between the different misalignment positions, while the Biodex system displayed significant differences across multiple misalignment position pairs.

## Discussion

This study presents an Alignment-Free Adaptive Joint Torque Measurement System (AFAJTM), which effectively addresses the alignment error issues inherent in traditional joint torque measurement methods, especially in the presence of joint misalignment. Unlike conventional methods that require precise alignment between the equipment's drive axis and the joint's axis of rotation, the AFAJTM utilizes an adaptive mechanism and adjustable linkage design to ensure that the measuring rod remains perpendicular to the limb throughout the joint torque measurement process. This system corrects for additional force components arising from alignment deviations automatically, enabling joint torque measurements without the required for alignment. By integrating this system into the EJTMD, experimental results validated that the system maintains high-precision torque measurements even at different misalignment positions.

In this study, the AFAJTM system estimates the position of the joint axis of rotation and the limb length automatically by combining indirect measurement methods with optimization algorithms, thereby avoiding the errors caused by visual alignment and manual measurements inherent in traditional methods. This adaptive algorithm not only improves measurement accuracy but also significantly reduces the requirement for alignment adjustments during operation, making the system particularly suitable for diverse joint measurement scenarios. Compared to previous systems that relied on direct torque measurements and strict alignment requirements, the AFAJTM system, with its alignment-free design and adaptive control mechanism, can provide accurate joint torque measurements even under various misalignment conditions, demonstrating strong adaptability and robustness. This system not only theoretically solves the alignment error problem inherent in traditional methods but also offers high modularity and flexibility, enabling it to be integrated as a module into any robotic system requiring joint torque measurement, further expanding its application scope.

Model experimental results demonstrate that the EJTMD's measurement accuracy and consistency were validated across different misalignment positions. First, paired t-test results (P-values ranging from 0.431 to 0.991) and regression analysis (regression coefficient 1.011,  $R^2 = 0.993$ ) indicate that there were no significant differences between the EJTMD's measurements and the standard values from the simulation model, and the measurements exhibited a good linear relationship, proving the accuracy and reliability of EJTMD as a joint torque measurement device. In the repeated measures ANOVA results for different misalignment positions indicate that there are no significant differences in the torque data between the five positions. Further paired t-tests also indicated no significant differences between the measurements at different misalignment positions (P-values all greater than 0.05), verifying that the EJTMD maintains consistency under different misalignment conditions. This suggests that the device and its underlying alignment-free adaptive model effectively counteract the impact of misalignment positions on the measurement results. The absolute error distribution between the EJTMD and the simulation model shown in Fig. 2 confirms the high accuracy of the torque measurements obtained from the EJTMD. Although the fitted limb length contributes significantly to the error, the overall error remains small, indicating that the measurement error of the EJTMD is within an acceptable range, further validating its high precision and reliability as a joint torque measurement device.

In the clinical experiments, the EJTMD showed high measurement consistency across different misalignment positions, with mean torque values ranging from 12.289 to 12.508 Nm and relatively small standard deviations (2.420 to 2.700 Nm). The intraclass correlation coefficients (ICCs) were all above 0.93, further confirming the high consistency of measurements. In contrast, the Biodex system exhibited significant variability, with torque measurements ranging from 10.379 to 17.343 Nm and larger standard deviations (4.625 to 5.140 Nm). The repeated measures ANOVA for the EJTMD showed that misalignment positions had no significant effect on measurements ( $F=0.119$ ,  $P=0.979$ ), indicating that the device remained stable regardless of position. However, for the Biodex system, misalignment positions significantly affected the measurements ( $F=46.071$ ,  $P<0.001$ ), reflecting its sensitivity to changes in position. Pairwise comparisons further revealed that the EJTMD showed no significant differences between misalignment positions, while the Biodex system displayed significant discrepancies in multiple comparisons. These results highlight the EJTMD's ability to provide stable and consistent torque measurements across a range of misalignment conditions, making it a reliable tool for joint torque measurement, especially in dynamic or misaligned settings. In contrast, the Biodex system showed significant misalignment sensitivity, which could introduce errors and affect measurement precision.

Although this study highlights many advantages of the AFAJTM system, some limitations remain. First, the study only conducted MVC experiments at specific angles, and a broader range of angles and torque values has yet to be tested. Therefore, the system's performance at other joint angles and higher torque levels requires further verification. Second, the sample size in this study was small, consisting of only ten healthy volunteers, and the sample diversity was limited. Future studies should aim to expand the sample size to include more diverse groups across various age ranges, body types, and health conditions. Additionally, the applicability of the AFAJTM system's alignment-free

measurement method in dynamic movements has not been fully validated, and future research could consider testing the system's performance in dynamic measurement environments. While the system performed reliably in controlled conditions, its real-world robustness requires further evaluation, as factors like environmental noise, sensor drift, and movement variability may affect accuracy. Future research could investigate the system's stability under prolonged usage and in more variable operational settings to enhance its practical applicability.

## Conclusions

In modern clinical settings, objectively and consistently measuring joint torque remains a complex and challenging task. Therefore, this study proposes an Alignment-Free Adaptive Joint Torque Measurement System, on the basis of which the EJTMD was developed. The device's effectiveness and consistency were tested to assess its feasibility for measuring joint torque under different misalignment conditions. The results demonstrate that the EJTMD provides high stability and consistency in measurements across various misalignment positions, with no significant impact from changes in misalignment. Additionally, comparisons between the EJTMD, joint simulation models, and clinical experiments validated its accuracy and repeatability. In contrast, the Biodex system's measurements were more sensitive to changes in misalignment positions, showing significant fluctuations. Therefore, the Alignment-Free Adaptive Joint Torque Measurement System offers a solution for joint torque measurement under misalignment conditions, improving measurement accuracy.

## Methods

### Design of the alignment-free adaptive joint torque measurement system

To avoid misalignment errors inherent in conventional torque measurement methods, torque can be indirectly calculated by measuring the force applied by the dynamometer and the distance from the measurement point to the joint's rotational axis, enabling adaptive torque measurement. Based on this approach, this study proposes an AFAJTM system, which is applicable to all joints that can be considered as rotating-hinge joints, such as the knee and elbow joints [28, 29]. The following section details the torque measurement system using the elbow joint as an example.

The schematic diagram of the AFAJTM structure is shown in the red portion of Fig. 4. Point B is equipped with an angle sensor to monitor the angle  $\beta$  between the linkage and the limb. Additionally, a force sensor is placed within the linkage AB to measure the force  $F$  applied along the direction of the linkage in real-time. These sensors are not limited to specific models and can be replaced with any suitable angle or force sensors. For example, potentiometers, magnetic encoders, and photoelectric encoders can be used to measure angles, while strain-based or piezoelectric force sensors are suitable for measuring the tensile force in the linkage AB. This design demonstrates that point A is designed to be flexible and adaptable, making it suitable for various types of torque-measuring mechanisms or devices, including exoskeleton robots that may require such measurements. The AFAJTM system thus provides a foundation for creating customizable and transplantable torque-measuring solutions.

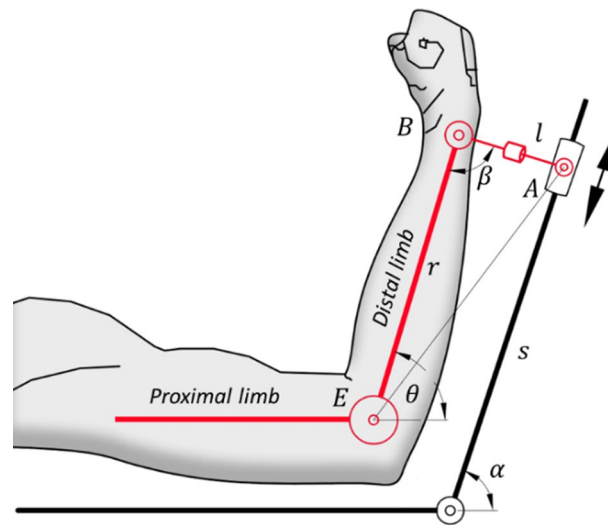


**Fig. 4** Schematic diagram of the AFAJTM structure. Point  $E$  represents the joint axis of rotation to be measured,  $BE$  represents the distal limb, and point  $B$  is the fixed connection between the linkage and the distal limb. Both ends of the linkage  $AB$  are equipped with a hinge joint with a single degree of freedom, where the axis of rotation for the rocker is  $O$ , and the slider is located on the rocker and connected to the linkage through a hinge. The length of the distal limb is  $r$ , the angle between the linkage and the distal limb is  $\beta$ , the joint flexion angle is  $\theta$ , the rotation angle of the rocker is  $\alpha$ , and the displacement of the slider is  $s$

Based on this model, the torque  $M$  at the joint is measured using the following equation:

$$M = F \cdot r \cdot \sin\beta + J \cdot \ddot{\theta} \tag{1}$$

where  $r$  is the distance between point  $B$  and the joint's rotational axis, i.e., the length of the distal limb,  $J$  is the moment of inertia of the moving limb about the joint's rotational axis, and  $\ddot{\theta}$  is the angular acceleration of the joint. This equation is derived from applying Newton's second law to the rotational system, where the total torque is the sum of the torques due to the applied force and the inertial resistance of the moving limb.

To evaluate the impact of measurement uncertainties on torque estimation, an uncertainty propagation analysis was conducted. The total torque uncertainty was computed as:

$$\delta M = \sqrt{(r\sin\beta\delta F)^2 + (F\sin\beta\delta r)^2 + (F\cos\beta\delta\beta)^2 + (\ddot{\theta}\delta J)^2 + (J\delta\ddot{\theta})^2} \tag{2}$$

where  $\delta F$ ,  $\delta r$ ,  $\delta\beta$ ,  $\delta J$ , and  $\delta\ddot{\theta}$  represent the uncertainties in force measurement, limb length, angle sensing, moment of inertia, and angular acceleration, respectively. The contribution of each uncertainty source was quantified as:

$$P_F = \frac{(r\sin\beta\delta F)^2}{\delta M^2}, P_r = \frac{(F\sin\beta\delta r)^2}{\delta M^2}, P_\beta = \frac{(F\cos\beta\delta\beta)^2}{\delta M^2}, P_J = \frac{(\ddot{\theta}\delta J)^2}{\delta M^2}, P_{\ddot{\theta}} = \frac{(J\delta\ddot{\theta})^2}{\delta M^2} \tag{3}$$

This analysis quantifies how uncertainties in force, limb length, angle measurement, moment of inertia, and angular acceleration propagate through the model, enabling

a systematic assessment of their impact on torque estimation accuracy and guiding improvements in measurement precision.

In the AFAJTM system, maintaining accurate force measurement is crucial. If the angle between the linkage and the limb deviates from the perpendicular (i.e.,  $\beta \neq 90^\circ$ ), a force along the limb's direction will be generated in the system, interfering with the force sensor measurement and causing the force data to deviate from the actual value. This effect, especially in precise force measurements, can significantly impact the accuracy of the results. Therefore, ensuring the linkage remains perpendicular to the limb is key to eliminating these unnecessary force components and improving measurement accuracy. To achieve this, the control system adjusts the end position to bring the angle  $\beta$  to the perpendicular state (i.e.,  $\beta = \pi/2$ ), thereby enabling precise control of the mechanical components. This adjustment process can be represented by:  $\beta_{des} = H(\Delta\beta)$ , where  $\beta_{des}$  is the target angle, and  $H(\Delta\beta)$  is the control function used to adjust the angle, with  $\Delta\beta$  representing the difference between the actual and target angles. The actual angle can be measured by the angle sensor at point B, and  $H$  is the controller's function to adjust the angle based on feedback. This adjustment is achieved using active devices with actuators, which are integrated into the control system to ensure real-time adjustments based on sensor feedback. Details about the control mechanism and actuator implementation are provided in the following sections.

In Eq. (1), the parameter  $r$ , the length of the limb, is difficult to measure accurately for any subject, as manual measurement typically involves significant errors. This study proposes a method to estimate  $r$  based on the AFAJTM system.

Define  $\{x_e, y_e\}$  represent the coordinates of the joint's axis of rotation, and  $\{x_a, y_a\}$  represent the coordinates of the module's connection point to the external robotic structure. Based on the kinematic relationship of the module, the following equation can be obtained:

$$l_{AE}^2 = (x_a - x_e)^2 + (y_a - y_e)^2 = l^2 + r^2 - 2rl\cos\beta \quad (4)$$

By constructing an optimization function and combining sensor data, a high-precision fitting of the coordinates of joint axis and limb length can be achieved. The state vector  $\mu_t = [x_e, y_e, r]^T$  is defined, based on Eq. (4), the optimization function  $f(\mu_t)$  is defined as follows:

$$f(\mu_t) = (x_a - x_e)^2 + (y_a - y_e)^2 - l^2 - r^2 + 2rl\cos\beta \quad (5)$$

Firstly, an initial value of the state vector  $\mu_0 = [x_{e,0}, y_{e,0}, r_0]^T$  is given, and a convergence threshold  $\epsilon$  is set to control the accuracy of the algorithm. Using gradient descent, the gradient of Eq. (5),  $\nabla f(\mu_t) = [\partial f/\partial x_e, \partial f/\partial y_e, \partial f/\partial r]^T$ , is computed to update the state vector at each iteration:  $\mu_{t+1} = \mu_t - \alpha \nabla f(\mu_t)$ .

where  $\alpha$  is the learning rate that adjusts the step size in each iteration. During the iteration process, the change in the state vector is continuously checked. When  $|\mu_{t+1} - \mu_t| < \epsilon$ , the iteration process converges, and the optimal solution  $\mu_t$  is obtained.

Through this iterative solution method, the system can fit the joint axis of rotation  $\{x_e, y_e\}$  and limb length  $r$  without misalignment errors. Additionally, to further improve estimation accuracy, the system can use multiple measurements from the sensors for

fitting and calibration, ensuring high-precision torque measurement throughout the entire joint movement range. This kinematics-based adaptive fitting method simplifies the alignment operation and meets the requirements for joint torque measurement under misalignment conditions, thus improving measurement accuracy.

**Adaptive motion trajectory control method based on AFAJTM**

In the planar AFAJTM system, the kinematic analysis of the elbow joint and the linkage can be modeled using the Denavit-Hartenberg (DH) parameter method.

Based on the modified D-H method<sup>30</sup> and the D-H parameters listed in Table 5, a corresponding homogeneous transformation matrix is established for each joint.  $T_0^1$  represents the transformation from the base coordinate system to the elbow joint, and  $T_1^2$  represents the transformation from the elbow joint to the end of the link.  $T_0^2$  represents the kinematic equation for the end of the link, which can be expressed as:

$$T_0^2 = T_0^1 \cdot T_1^2 \tag{6}$$

The coordinates  $\{x_a, y_a\}$  of the end of the linkage are:

$$\begin{cases} x_a = x_e + r\cos\theta + l\cos(\theta + \beta) \\ y_a = y_e + r\sin\theta + l\sin(\theta + \beta) \end{cases} \tag{7}$$

The  $\{x_a, y_a\}$  coordinates are provided by the embedded end robot.

For any device integrated with the AFAJTM, a control method is proposed to drive the limb along a predefined trajectory based on different force measurement modes. The predefined motion trajectory of the limb is represented by  $\theta_{target}$ , and the AFAJTM end coordinates trajectory can be expressed as  $\{x_a, y_a\} = f(\theta_{target}, \beta, x_e, y_e, r, l)$ , which is a function of the input predefined trajectory  $\theta_{target}$ , the angle  $\beta$ , the joint axis coordinates  $\{x_e, y_e\}$ , the linkage length  $l$ , and the limb length  $r$ .

Thus, the control of the limb’s motion trajectory is transformed into the control of the device’s end-effector trajectory.

**Elbow joint torque measurement device using AFAJTM**

This study designs an elbow joint torque measurement device (EJTMD) based on AFAJTM. As shown in Fig. 4, the end of the AFAJTM integrates an RP (Rotary and Prismatic) robotic arm, which is connected to the AFAJTM at point A. The core components of the device include a rocker, a slider, and the AFAJTM. Specifically, as shown in Fig. 5a and b, the rocker is driven by a belt drive system controlled by the state variable  $\alpha$ ; the slider moves along a linear rail installed on the rocker, and the prismatic joint is controlled by a servo motor via the belt drive system. The slider is equipped with a displacement sensor to measure the displacement  $s$ .

**Table 5** EJTMD Chain’s D-H parameters

$i$	$\alpha_{i-1}$	$a_{i-1}$	$d_i$	$\theta_i$
1	0	$r$	0	$\theta$
2	0	$l$	0	$\beta$

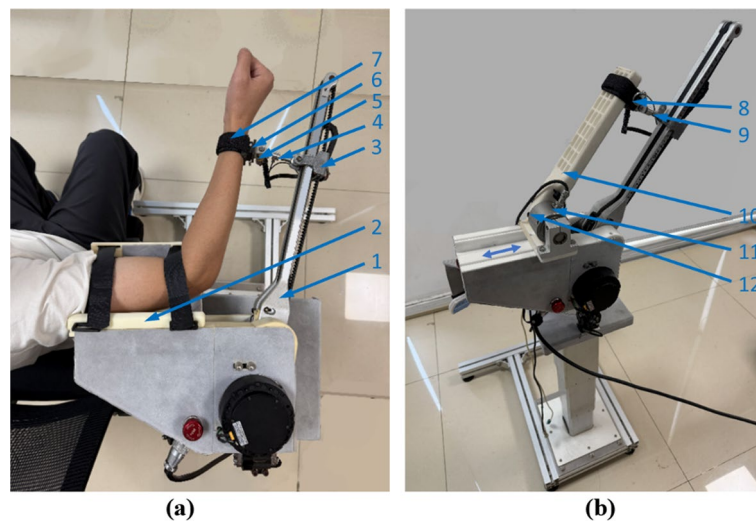


**Fig. 5** Experimental setup of EJTMD: **a** Clinical experiment setup; **b** Model experiment setup. Key components include: 1. Rocker, 2. Movable elbow support (X-direction: movement direction parallel to axis), 3. Slider, 4. Linkage, 5. Micro angle encoder, 6. Semicircular ring, 7. Velcro straps, 8. Pin, 9. Force sensor, 10. Limb simulation model, 11. Torque sensor, 12. Angle encoder

The end of the AFAJTM's linkage is hinged to the slider, while the other end is connected to a semicircular padded metallic structure via a hinge, which is designed to secure the subject's limb. The structure is equipped with an angle encoder to monitor the angle between the linkage and the limb in real-time. The semicircular ring features a quick-release system, allowing for rapid detachment from the rod by removing the pin. The ring is fixed to the limb using Velcro straps.

The force sensor (SBT641, 5 kg, 0.3%, SimBaTouch Electronic Technology Co., Ltd.) and the micro angle encoder (PD1503, 0–360°, 17bit, Pudi Electronic Co., Ltd.) are sampled at a frequency of 1 kHz on a 32-bit microprocessor (STM32F4, 168 MHz), which is programmed using the STM32CubeIDE environment. The microprocessor communicates with the servo motors (PM10025, 6 Nm, SteadyWin Equipment Co., Ltd.) via CAN bus, utilizing a dedicated CAN communication library for data exchange. Advanced control loops, data logging, and user communication are managed by a Raspberry Pi 4B operating at 500 Hz, running a Raspbian OS.

The custom GUI for data monitoring and parameter selection is developed in Python using PyQt for the graphical interface. This GUI communicates with the Raspberry Pi via an Ethernet connection using a TCP/IP protocol, allowing real-time monitoring of the system's status and dynamic adjustment of experimental parameters. The GUI also logs data locally for post-experiment analysis. The software includes various configurations for initializing the system, such as setting the CAN bus parameters and SPI communication rates between the Raspberry Pi and the STM32F4.

To ensure test safety, three emergency stop mechanisms are designed. First, if the force exceeds the preset range of  $\pm 120\text{N}$ , the software will automatically control the delay of the two servo motors. Second, if the rotation angle exceeds the preset range, the motor will stop automatically. Additionally, both the operator and the subject can

press an emergency stop button at any time during the test, cutting off power to the two servo motors to protect the subject's joint.

#### **Torque consistency evaluation of the EJTMd at misalignment positions (model experiment)**

To evaluate the torque measurement consistency and repeatability of the self-designed EJTMd under different misalignment conditions in a controlled environment, a joint simulation model was designed (as shown in Fig. 5b). The coordinate system used in the simulation is defined with its origin at the axis of rotation of the rocker. The X-direction is parallel to the movable elbow support, while the Y-direction is perpendicular to the movable elbow support. The model is equipped with a torque sensor (JNNT-S) and an angle encoder (PD1503, Pudi Electronic Co., Ltd.) at the joint to monitor the joint torque and angle variations in real time. To simulate joint misalignments, the joint simulation model is mounted on a movable elbow support, allowing the model joint to generate a quantitative displacement in the X-direction.

The experiment is conducted out by setting the joint angle of the simulation model at 90° and locking it to the base. Subsequently, the misalignment of the joint axis is gradually adjusted to observe the influence of different misalignment positions on the torque measurement. The origin of the system's coordinate axis is set at the axis of rotation of the rocker, and the misalignment positions in the XY plane are set as (− 50, 0), (− 30, 0), (0, 0), (0, 30), and (0, 50), as shown in Fig. 5b. The (0, 0) position indicates that the misalignment coordinates of the model's joint axis relative to the rocker's axis of rotation of EJTMd are (− 60, 40), with units in millimeters. The other four positions are moved relative to the (0, 0) position.

At each misalignment position, the EJTMd randomly applies a tensile force of 10 to 20 Nm, conducting 30 MVC experiments, each lasting 4 s. During the experiment, torque data is recorded when the simulation model and the EJTMd reach a stable stage. Specifically, when the torque fluctuation is within  $\pm 0.5$  Nm and remains stable, the torque data for that stage is recorded (as shown in Fig. 6), and the average value is calculated, denoted as  $\tau_{model}$  and  $\tau_{EJTMd}$ , respectively.

#### **Comparison of torque measurements between EJTMd and Biodex system at misalignment positions (clinical experiment)**

The purpose of this experiment was to evaluate the consistency of joint torque measurements between the EJTMd and the standard dynamometer (Biodex system) at different misalignment positions, by comparing the isometric maximum voluntary contraction (MVC) results.

A total of 10 healthy volunteers (age:  $26.35 \pm 3.7$  years, height:  $172.6 \pm 7.50$  cm, weight:  $66.9 \pm 8.85$  kg, including 3 females, 7 males, 2 left-handed, and 8 right-handed) were recruited for the experiment. Each participant performed three consecutive MVC tests at five different misalignment positions using both the EJTMd and the Biodex system. Participants performed isometric contractions (static force exertion) with the elbow fixed at 90° flexion (0° = full extension), following standardized instructions: 'Push as hard as possible against the device for 4 s'. Each test lasted for 4 s, and the average torque value during the stable phase was recorded. The three

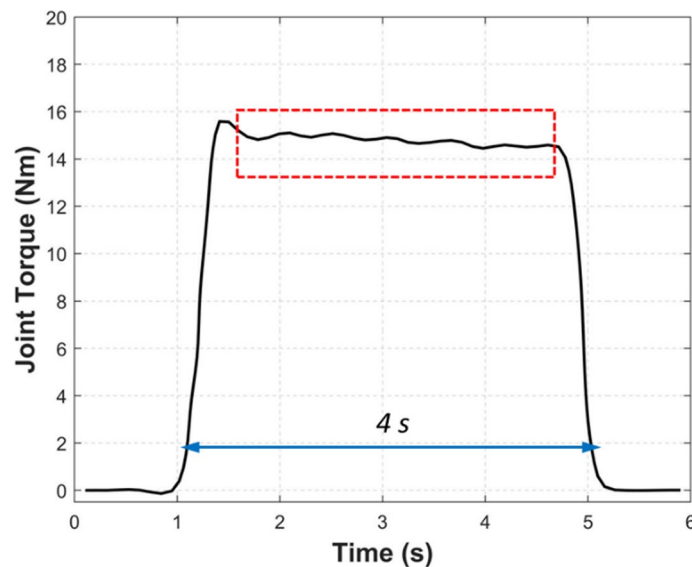


**Fig. 6** A sample of EJTMD torque waveform. Red dashed box: The target torque was chosen for the analysis

trials at each position were performed sequentially, with a 30 s rest period was provided between each test to avoid muscle fatigue. To minimize learning effects, participants completed 3 submaximal practice trials (50% effort) at the neutral position (0,0) before formal testing. To ensure the reliability of the results, a rotating testing procedure was used, where different volunteers tested at random assigned starting misalignment positions and were allowed sufficient rest if feeling fatigued. The order of testing devices (EJTMD/Biodex) and misalignment positions was randomized across participants.

For the EJTMD testing, the participants sat on the seat, with their upper arm placed on the elbow support, and the elbow joint was set to  $90^\circ$ , as shown in Fig. 5a. The trunk was stabilized with a chest strap to prevent compensatory movements. Five different misalignment positions were simulated in the XY plane relative to the humeral lateral epicondyle with coordinates:  $(-50, 0)$ ,  $(-30, 0)$ ,  $(0, 0)$ ,  $(0, 30)$ , and  $(0, 50)$  mm. The setup of these five positions was the same as in the joint simulation model. The upper arm was secured to the elbow support with Velcro straps, as close as possible to the rotation axis of the rocker, and kept parallel to the forearm plate. The elbow joint axis of rotation did not need to align with the rocker axis. The forearm and wrist were connected to the EJTMD via Velcro straps.

For the Biodex system, the upper body of the participants was secured at the chest to minimize interference from other body parts. The elbow joint was positioned at  $90^\circ$  for the standardized MVC test. The alignment of the dynamometer's probe with the lateral epicondyle of the humerus indicates alignment between the rotation axis of the dynamometer and the joint axis of rotation, labeled as position  $(0, 0)$ , and the lever arm pad was positioned within 2 cm of the wrist joint. Real-time visual feedback of torque was displayed on a monitor to guide maximal effort. The misalignment positions in the XY plane were consistent with those in the EJTMD testing:  $(-50, 0)$ ,  $(-30, 0)$ ,  $(0, 0)$ ,  $(0, 30)$ , and  $(0, 50)$  mm.

Torque signals from both devices were filtered offline using a 4th-order Butterworth low-pass filter (cutoff frequency: 10 Hz).

### Statistical analysis

All measurement data were continuous variables and were described using mean and variance. Normality was tested using the Shapiro–Wilk test. For the simulation experiment data, regression analysis was first used to investigate the effect of applied force on the EJTMD measurement results, examining the correlation between applied force and measured torque. Then, we selected five specific positions and used correlation analysis and independent samples t-test to evaluate the differences between the EJTMD measurements ( $\tau_{EJTMD}$ ) and the standard values from the joint simulation model ( $\tau_{model}$ ). The absolute error distribution between the EJTMD and the Simulation Model was analyzed, and the contributions of force sensor, limb length, and angle measurement errors were quantified. The measurement consistency of the EJTMD system at each misalignment position was assessed using the intraclass correlation coefficient (ICC). A repeated measures analysis of variance (RM-ANOVA) was performed for both devices to assess the effect of misalignment position on torque measurements. Mauchly's test was used to check sphericity, and when violated ( $P < 0.05$ ), degrees of freedom were adjusted using the Greenhouse–Geisser or Huynh–Feldt corrections. Post hoc Bonferroni-corrected pairwise comparisons were conducted to assess differences between positions. Data analysis was conducted using SPSS 22 (IBM, USA).

### Author contributions

LL contributed to methodology, investigation, data analysis, and writing—original draft, as well as mechanical and electrical design and assembly. JC contributed to resources and investigation. SS was involved in resources, review, and project administration. WP was involved in conceptualization and project administration. All authors read and approved the final manuscript.

### Funding

This research was funded by Anhui Provincial Key Research and Development Project (202304a05020078).

### Availability of data and materials

No datasets were generated or analysed during the current study.

### Declarations

#### Ethics approval and consent to participate

All experiment procedures covered in this study were evaluated and approved by the Ethic Committee of the Affiliated Hospital of Institute of Neurology, Anhui University of Chinese Medicine.

#### Consent for publication

Not applicable.

#### Competing interests

The authors declare no competing interests.

Received: 23 December 2024 Accepted: 18 February 2025

Published online: 24 February 2025

### References

1. Urhausen AP, Berg B, Øiestad BE, et al. Measurement properties for muscle strength tests following anterior cruciate ligament and/or meniscus injury: what tests to use and where do we need to go? A systematic review with meta-analyses for the OPTIKNEE consensus. *Br J Sports Med.* 2022;56(24):1422–31.
2. Liu K, Delaney AN, Kaminski TW. A review of the role of lower-leg strength measurements in ankle sprain and chronic ankle instability populations. *Sports Biomech.* 2022;21(4):562–75.

3. Sin M, Kim WS, Cho K, et al. Improving the test-retest and inter-rater reliability for stretch reflex measurements using an isokinetic device in stroke patients with mild to moderate elbow spasticity. *J Electromyogr Kinesiol.* 2018;39:120–7.
4. Averta G. A novel mechatronic system for evaluating elbow muscular spasticity relying on tonic stretch reflex threshold estimation //human-aware robotics: modeling human motor skills for the design, planning and control of a new generation of robotic devices. Cham: Springer International Publishing; 2022. p. 127–39.
5. Zemková E. Strength and power-related measures in assessing core muscle performance in sport and rehabilitation. *Front Physiol.* 2022;13:861582.
6. Tourillon R, Michel A, Fourchet F, et al. Human foot muscle strength and its association with sprint acceleration, cutting and jumping performance, and kinetics in high-level athletes. *J Sports Sci.* 2024. <https://doi.org/10.1080/02640414.2024.2367365>.
7. Yilmaz S, Erdemir İ. The influence of quadriceps and hamstring strength on balance performance. *Phys Educ Stud.* 2023;27(3):112–7.
8. Forrester SE, Yeadon MR, King MA, et al. Comparing different approaches for determining joint torque parameters from isovelocity dynamometer measurements. *J Biomech.* 2011;44(5):955–61.
9. Haugland M, Ramos-Murguialday A, Hultborn H, et al. Measuring resistance to externally induced movement of the wrist joint in chronic stroke patients using an objective hand-held dynamometer. *Clin Neurophysiol Pract.* 2023;8:97–110.
10. Ancillao A, Rossi S, Cappa P. Analysis of knee strength measurements performed by a hand-held multicomponent dynamometer and optoelectronic system. *IEEE Trans Instrum Meas.* 2016;66(1):85–92.
11. Tsaopoulos DE, Baltzopoulos V, Richards PJ, et al. Mechanical correction of dynamometer moment for the effects of segment motion during isometric knee-extension tests. *J Appl Physiol.* 2011;111(1):68–74.
12. Janssen JC, Le-Ngoc L. Intratester reliability and validity of concentric measurements using a new hand-held dynamometer. *Arch Phys Med Rehabil.* 2009;90(9):1541–7.
13. Sørensen L, Oestergaard LG, Van Tulder M, et al. Measurement properties of handheld dynamometry for assessment of shoulder muscle strength: a systematic review. *Scand J Med Sci Sports.* 2020;30(12):2305–28.
14. McCabe MV, Van Citters DW, Chapman RM. Developing a method for quantifying hip joint angles and moments during walking using neural networks and wearables. *Comput Methods Biomech Biomed Engin.* 2023;26(1):1–11.
15. Faber GS, Kingma I, Chang CC, et al. Validation of a wearable system for 3D ambulatory L5/S1 moment assessment during manual lifting using instrumented shoes and an inertial sensor suit. *J Biomech.* 2020;102:109671.
16. Ivarsson A, Cronström A. Agreement between isokinetic dynamometer and hand-held isometric dynamometer as measures to detect lower limb asymmetry in muscle torque after anterior cruciate ligament reconstruction. *Int J Sports Phys Ther.* 2022;17(7):1307.
17. Van der Woude DR, Ruyten T, Bartels B. Reliability of muscle strength and muscle power assessments using isokinetic dynamometry in neuromuscular diseases: a systematic review. *Phys Ther.* 2022;102(10):pzac099.
18. Rosales-Luengas Y, Espinosa-Espejel KI, Lopéz-Gutiérrez R, et al. Lower limb exoskeleton for rehabilitation with flexible joints and movement routines commanded by electromyography and baropodometry sensors. *Sensors.* 2023;23(11):5252.
19. Alvares JBAR, Rodrigues R, de Azevedo FR, et al. Inter-machine reliability of the Biodex and Cybex isokinetic dynamometers for knee flexor/extensor isometric, concentric and eccentric tests. *Phys Ther Sport.* 2015;16(1):59–65.
20. Kocahan T, Akinoğlu B, Yilmaz AE, et al. Intra- and inter-rater reliability of a well-used and a less-used IsoMed 2000 dynamometer for knee flexion and extension peak torque measurements in a concentric test in athletes. *Appl Sci.* 2021;11(11):4951.
21. MajidiRad AH, Yihun Y, Hakansson N, et al. The effect of lower limb exoskeleton alignment on knee rehabilitation efficacy. *Healthcare MDPI.* 2022;10(7):1291.
22. Houweling TAW, Hamzeh MA. Does knee joint alignment with the axis of the isokinetic dynamometer affect peak torque? *Isokinet Exerc Sci.* 2010;18(4):217–21.
23. Reimann U, Verdonck AJ, Wiek M. The influence of a joint displacement on torque, angle and angular velocity during isokinetic knee extension/flexion. *Theor ConSID Isokinetics Exerc Sci.* 1997;6(4):215–21.
24. Arampatzis A, Karamanidis K, De Monte G, et al. Differences between measured and resultant joint moments during voluntary and artificially elicited isometric knee extension contractions. *Clin Biomech.* 2004;19(3):277–83.
25. Vitiello N, Cempini M, Crea S, et al. Functional design of a powered elbow orthosis toward its clinical employment. *IEEE/ASME Trans Mechatron.* 2016;21(4):1880–91.
26. Li G, Liang X, Lu H, et al. Development and validation of a self-aligning knee exoskeleton with hip rotation capability. *IEEE Trans Neural Syst Rehabil Eng.* 2024. <https://doi.org/10.1109/TNSRE.2024.3354806>.
27. Schorsch JF, Keemink AQL, Stienen AHA, et al. A novel self-aligning mechanism to decouple force and torques for a planar exoskeleton joint. *Mech Sci.* 2014;5(2):29–35.
28. Afifi M, Abdulazeez MU, Aminian K, et al. A protocol for obtaining upper and lower extremity joints' range of motion in children using three-dimensional motion analysis system. *Front Physiol.* 2024;15:1416175.
29. Aquilina AL, Grazette AJ. Clinical anatomy and assessment of the elbow. *Open Orthop J.* 2017;11:1347–52.
30. Li G, Cheng L, Gao Z, et al. Development of an untethered adaptive thumb exoskeleton for delicate rehabilitation assistance. *IEEE Trans Rob.* 2022;38(6):3514–29.

## Publisher's Note

Springer Nature remains neutral with regard to jurisdictional claims in published maps and institutional affiliations.